The Journal of Neuroscience, November 1, 1997, 17(21):8213–8224

Alternative Splicing in the Pore-Forming Region of *shaker* Potassium Channels

Marshall Kim,[1] Deborah J. Baro,[1] Cathy C. Lanning,[1] Mehul Doshi,[1] Jeremy Farnham,[1] Howard S. Moskowitz,[1] Jack H. Peck,[2] Baldomero M. Olivera,[3] and Ronald M. Harris-Warrick[1]

[1]Section of Neurobiology and Behavior, Cornell University, Ithaca, New York 14853, [2]Department of Psychology, Ithaca College, Ithaca, New York 14850, and [3]Department of Biology, University of Utah, Salt Lake City, Utah 84112

We have cloned cDNAs for the *shaker* potassium channel gene from the spiny lobster *Panulirus interruptus*. As previously found in *Drosophila*, there is alternative splicing at the 5′ and 3′ ends of the coding region. However, in *Panulirus shaker*, alternative splicing also occurs within the pore-forming region of the protein. Three different splice variants were found within the P region, two of which bestow unique electrophysiological characteristics to channel function. Pore I and pore II variants differ in voltage dependence for activation, kinetics of inactivation, current rectification, and drug resistance. The pore 0 variant lacks a P region exon and does not produce a functional channel. This is the first example of alternative splicing within the pore-forming region of a voltage-dependent ion channel. We used a recently identified potassium channel blocker, κ-conotoxin PVIIA, to study the physiological role of the two pore forms. The toxin selectively blocked one pore form, whereas the other form, heteromers between the two pore forms, and *Panulirus shal* were not blocked. When it was tested in the *Panulirus* stomatogastric ganglion, the toxin produced no effects on transient K^+ currents or synaptic transmission between neurons.

Key words: potassium channel; shaker*; stomatogastric; pore-forming region; alternative splicing; conotoxin*

Transient voltage-dependent potassium currents (I_A) play a critical role in shaping the electrical activity of neurons, helping to regulate action potential shape, tonic spike frequency, transmitter release, and rhythmic bursting (Serrano and Getting, 1989; Hille, 1992; Tierney and Harris-Warrick, 1992; Harris-Warrick et al., 1995). I_A is not a uniform current, but it can be expressed with different properties (Wei et al., 1990). Different neurons can show markedly different types of I_A, with varying maximal conductance, voltage dependence, and degree and rate of inactivation (Pfaffinger et al., 1991; Furakawa et al., 1992; Baro et al., 1996b). This helps neurons to have different intrinsic electrophysiological properties. At least part of this I_A diversity arises from complexity in gene expression for these channels (Baro et al., 1996a, 1997).

In *Drosophila*, the transient K^+ current is generated by the *shaker* and *shal* members of the *Shaker* family of potassium channels (Wu and Haugland, 1985; Papazian et al., 1987; Iverson et al., 1988; Kamb et al., 1988; Pongs et al., 1988; Timpe et al., 1988; Stocker et al., 1990; Wei et al., 1990). The *Drosophila shaker* subfamily transcript undergoes alternative splicing at the 5′ and 3′ ends of the coding region, with five alternative 5′ ends and two alternative 3′ ends (Kamb et al., 1988; Pongs et al., 1988; Schwarz et al., 1988). This alternative splicing generates up to 10 different proteins that form markedly different ion channel types, from rapidly inactivating A-type currents to slowly or noninactivating delayed rectifier-type currents. Functional channels are composed of tetramers of *shaker* proteins (Isacoff et al., 1990; MacKinnon, 1991), and heteromers can also be produced between the alternate splice forms of *shaker*, generating further diversity in channel types (Isacoff et al., 1990; McCormack et al., 1990; Ruppersberg et al., 1990; MacKinnon, 1991; Sheng et al., 1993; Wang et al., 1993). In *Drosophila*, all of these splice variants share a common conserved core region, which extends from before the first transmembrane region (S1) to the end of the pore-forming P region (Kamb et al., 1988; Pongs et al., 1988; Schwarz et al., 1988). Ion flux occurs through the P region, and site-directed mutagenesis of the amino acid sequence of this region has important functional consequences (MacKinnon et al., 1988; MacKinnon and Miller, 1989; MacKinnon and Yellen, 1990; Hartmann et al., 1991; Yellen et al., 1991; Yool and Schwarz, 1991; Heginbotham and MacKinnon, 1992). The P region forms a loop that extends into the center of the pore, with the four pore loops of the subunits forming the selectivity filter (MacKinnon, 1995; Gross and MacKinnon, 1996; Ranganathan et al., 1996).

We have cloned the *shaker* homolog from the spiny lobster *Panulirus interruptus*, with the eventual goal of correlating the characteristics of the cloned channels with those of endogenous potassium currents in identified neurons from this species. In addition to alternative splicing at the 5′ and 3′ ends as in *Drosophila*, *Panulirus shaker* shows alternative splicing of the pore-lining P region, resulting in markedly different current properties.

MATERIALS AND METHODS

Screening cDNA libraries

We isolated *Panulirus shaker* sequences by PCR screening of five cDNA libraries, using materials and methods described in Baro et al. (1996b). In addition to the four cDNA libraries described in Baro et al. (1996b), one cDNA library made from mixed (abdominal, cerebral, and thoracic)

Received June 12, 1997; revised Aug. 15, 1997; accepted Aug. 21, 1997.

This work was supported by National Institutes of Health Grants NS25915, NS35631, and NS17323 (to R.H.W.); Grant GM 48677 (to B.M.O.); and a Hughes undergraduate fellowship (to M.D.). We thank Bruce Johnson, Robert Levini, Lauren French, David Deitcher, David McCobb, and Thomas Podleski for comments on this manuscript.

Correspondence should be addressed to Dr. Ronald Harris-Warrick, Section of Neurobiology and Behavior, Cornell University, Seeley G. Mudd Hall, Ithaca, NY 14853.

Table 1. Voltage dependence of activation and inactivation for B(I), B(II), B(I/II)

Clone	$V_{1/2\ activ}$ (mV)	$Slope_{act}$ (mV)	$V_{1/2\ inact}$ (mV)	$Slope_{inact}$ (mV)
B(I)	$-46.4 \pm 0.7^{b,c}$	$14.0 \pm 0.3^{b,c}$	-44.2 ± 0.4^{c}	3.4 ± 0.1^{b}
	$n = 16$	$n = 16$	$n = 16$	$n = 16$
B(II)	$-31.7 \pm 0.4^{a,c}$	$22.6 \pm 0.5^{a,c}$	-43.9 ± 0.4^{c}	$2.9 \pm 0.1^{a,c}$
	$n = 23$	$n = 23$	$n = 26$	$n = 26$
B(I/II)	$-39.6 \pm 0.9^{a,b}$	$25.7 \pm 0.9^{a,b}$	$-42.2 \pm 0.6^{a,b}$	3.3 ± 0.1^{b}
	$n = 10$	$n = 10$	$n = 10$	$n = 10$

[a]Significantly different from B(I) ($p < 0.05$).
[b]Significantly different from B(II) ($p < 0.05$).
[c]Significantly different from B(I/II) ($p < 0.05$).

ganglia RNA was kindly provided by W. Krenz and A. I. Selverston (University of California, San Diego, CA). The libraries were plated at a density of 5×10^4 pfu/150 mm plate, overlaid with 10 ml of SM buffer, and the phage lysate was collected. Then the phage lysates were used in PCRs with 5 μl of phage lysate from each plate and two *shaker* primers: 5′ primer, 5′ TCACTACCCAAGCTAAGTAGCCAGG 3′; and 3′ primer, 5′ CTCTCGCAGAAGTCGTGGT 3′. Small segments of *Panulirus shaker*-specific sequences were obtained using degenerate primers in RT-PCRs as described in Baro et al. (1994). The location of these primers is indicated in Figure 2.

The PCR products were run on an agarose gel to check for the presence of the *shaker*-specific 107 bp band. To plaque-purify the positive clone in the plate lysate, we performed conventional screening, using the ^{32}P-labeled 107 bp PCR fragment on plaques transferred to nylon membranes. Then the plaque-purified clones were rescued and sequenced as described in Baro et al. (1996b).

Reverse transcription-PCR (RT-PCR)

To determine whether the cloned sequences are expressed in RNA, we made cDNA from 1 μg of combined ganglia RNA in a standard reverse transcription reaction (Sambrook et al., 1989). The S4–S6 region of *shaker* was amplified from the cDNA in a PCR with the following primers: 5′ RT-PCR primer, 5′ AGCGATGGCACACAGGGA 3′; and 3′ RT-PCR primer, 5′ GCACGAGAAGGGGTCAAACC 3′.

The products were run on an 8% acrylamide gel. The PCR products were gel-purified, blunt-ended, kinased, subcloned into pBluescript, and sequenced to verify their identities (Baro et al., 1994).

Xenopus *oocyte studies*

The *Xenopus* oocyte expression studies were performed as described previously by Baro et al. (1996b). RNA was transcribed from linearized DNA templates with either T3 or T7 RNA polymerase. One hundred nanoliters of RNA (0.1 μg/μl) were injected into *Xenopus* oocytes, which were incubated in ND96 containing (in mM) 96 NaCl, 2 KCl, 1.8 $CaCl_2$, 1 $MgCl_2$, and 5 HEPES, pH 7.6, plus 5% fetal bovine serum at 18°C for 2–4 d. For the heteromer studies a 1:1 ratio of B(I) and B(II) RNA was injected. The two-electrode voltage-clamp recordings were performed in ND96 solution with protocols and data analysis performed using pClamp software (Axon Instruments, Foster City, CA) as described previously by Baro et al. (1996b) except that oocytes were held at −70 mV and no prepulse was given for any protocol, except for the voltage dependence of inactivation. The current signal was filtered at 1000 Hz.

Voltage dependence of activation. A series of 300 msec steps from −60 to +50 mV in 10 mV increments was given from a V_{hold} of −70 mV. The peak current of each step was converted to conductance by using a V_{rev} of −94 mV. Then the values were fit by the Boltzmann relation:

$$g(V) = g_{max}/[(1 + e^{-((V_{1/2}-V)/s)})^n], \quad (1)$$

where $g(V)$ is the peak conductance at a given voltage, g_{max} is the maximal conductance, $V_{1/2}$ is the voltage at which one-half of the gating particles are in an open configuration, V is the voltage, s is the e-fold slope factor, and $n = 3$.

Gating charge. The gating charge, z, was calculated by the method of limiting slopes, as described by Logothetis et al. (1992). We plotted the $ln(g/g_{max})$ versus voltage for the activation curves and determined the slope in the central linear region. The slope was fit by the equation:

$$z = RT/F[ln(g/g_{max})]/V. \quad (2)$$

Voltage dependence of inactivation. A series of 10 sec prepulses ranging from −80 to −10 mV was given before a 300 msec activating step to +20 mV, and the peak conductance during the +20 mV step was calculated. Then the values were fit by the Boltzmann equation, with $n = 1$.

Kinetics of inactivation at +20 mV A step was given from a V_{hold} of −70 to +20 mV for 6 sec, and the falling phase of the current trace was fit with the following third-order equation, using pClamp software:

$$I(t) = I_0 + I_{fast}e^{-t/\tau_{fast}} + I_{int}e^{-t/\tau_{int}} + I_{slow}e^{-t/\tau_{slow}}, \quad (3)$$

where τ_{fast}, τ_{int}, and τ_{slow} are the time constants of inactivation, I_{fast}, I_{int}, and I_{slow} are the amplitudes of the current components, and I_o is the amplitude of current that does not inactivate with time.

Activation rate at +20 mV A 30 msec step was given from −70 to +20 mV, and the time-to-peak current amplitude was measured.

Reversal potential. Tail currents were obtained by giving an activating step to +20 mV, followed by a series of repolarizing steps in 5 mV increments to various potentials depending on the external K^+ concentration (2, 10, and 50 mM external K^+, in which the Na^+ was replaced by K^+). The instantaneous tail currents were normalized and plotted against voltage.

κ-Conotoxin PVIIA studies. κ-Conotoxin PVIIA from *Conus purpurascens* was diluted to varying final concentrations in ND96 recording solution. Oocytes were recorded from a well with 200 μl of ND96. Steps were given to +20 mV, and the peak current was measured to obtain a baseline. The peak current was measured at 1 min intervals while the conotoxin concentration was successively increased in 10 min steps to allow for equilibration of toxin binding. To determine the IC_{50} value, we fit the dose–response curve data with the equation: $y = (1 + (T/IC_{50}))^{-1}$, where y = normalized current and T = toxin concentration.

Statistics. Student's t tests were performed assuming unequal variances for the data in Tables 1 and 2, using Excel software (Microsoft, Redmond, WA).

Electrophysiology of pyloric neurons

To study the effects of κ-conotoxin PVIIA on pyloric neurons, we measured I_A in various pyloric neurons, as described previously (Harris-Warrick et al., 1995), in the presence of 2 μM κ-conotoxin PVIIA. The effects of the toxin on spike-evoked synaptic transmission were measured by current-clamping two neurons (as described in Johnson et al., 1995), delivering a depolarizing step into one neuron to evoke a spike, and measuring the amplitude of the postsynaptic inhibitory potential in the other neuron in the presence of 1 μM toxin. Signal averaging was used, with the presynaptic spike as the trigger.

RESULTS

Alternative splicing in *Panulirus shaker*

To clone cDNAs for *Panulirus shaker*, we screened $>5 \times 10^6$ plaques from five *Panulirus* cDNA libraries derived from abdominal, thoracic, and cerebral ganglia RNA, as described previously (Baro et al., 1996b). Figure 1*A* shows three cDNA clones that

Table 2. Kinetics of activation and inactivation for B(I), B(II), B(I/II)[a]

Clone	Time to peak (msec)	τ_{fast} (msec)	Percentage	τ_{int} (msec)	Percentage	τ_{slow} (msec)	Percentage	Noninact (%)
B(I)	6.8 ± 0.2[d]	12.9 ± 0.3[c]	50.4 ± 0.9[c,d]	535 ± 25[c,d]	9.4 ± 0.8[c]	1833 ± 51[c,d]	25.2 ± 0.9[c]	15.0 ± 1.2[c]
	n = 17	n = 14	n = 14	n = 16	n = 16	n = 16	n = 16	n = 16
B(II)	6.6 ± 0.2[d]	9.2 ± 0.2[b,d]	74.7 ± 1.5[b,d]	112 ± 15[b,d]	6.1 ± 0.6[b,d]	968 ± 44[b,d]	12.9 ± 0.9[b,d]	6.4 ± 0.2[b,d]
	n = 19	n = 19	n = 19	n = 13	n = 13	n = 13	n = 13	n = 13
B(I/II)	8.7 ± 0.4[b,c]	12.2 ± 0.6[c]	58.6 ± 3.2[b,c]	213 ± 46[b,c]	9.0 ± 0.7[c]	1469 ± 50[b,c]	21.0 ± 2.4[c]	11.4 ± 0.5[b]
	n = 10	n = 10	n = 10	n = 10	n = 10	n = 10	n = 10	n = 10

[a]Measurements made during a step to +20 mV.
[b]Significantly different from B(I) ($p < 0.05$).
[c]Significantly different from B(II) ($p < 0.05$).
[d]Significantly different from B(I/II) ($p < 0.05$).

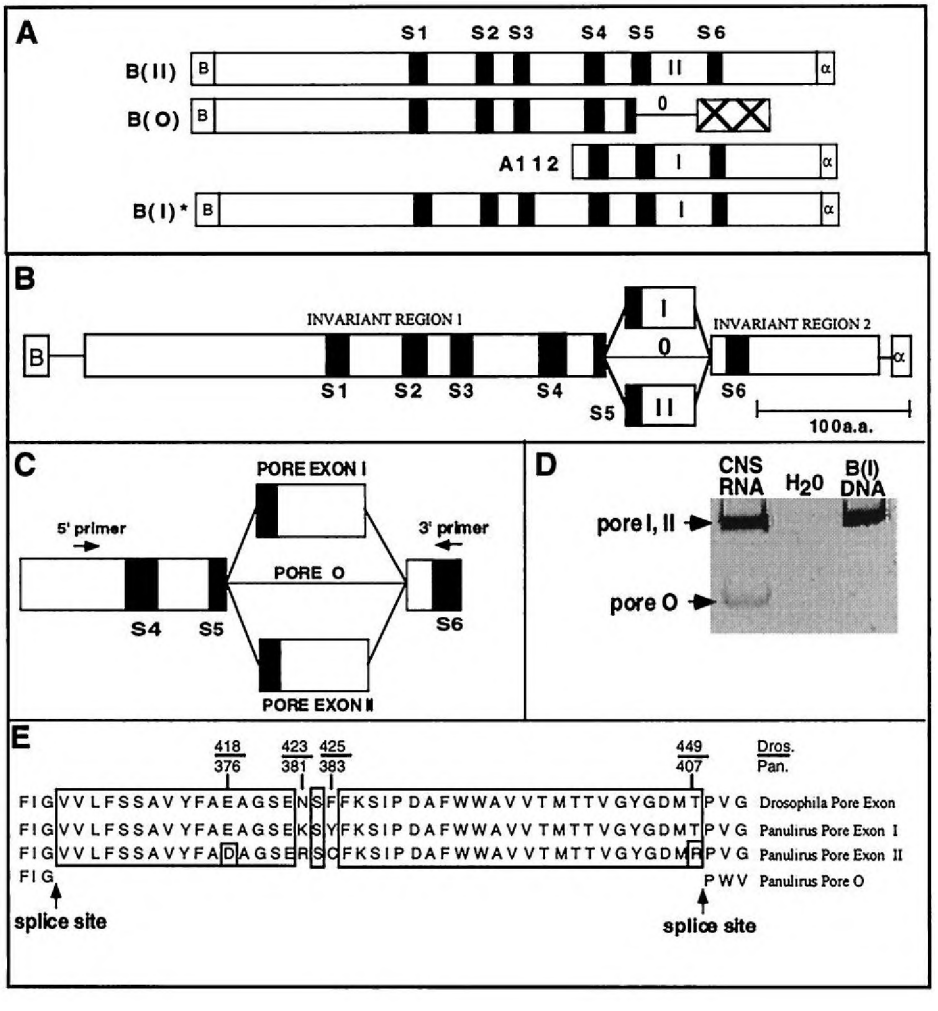

Figure 1. Alternative splicing in *Panulirus shaker*. *A*, Summary of the cDNA clones used in this study. Clones B(II) and B(0) contained complete open reading frames (ORFs). The absence of an exon in the P region of B(0) caused a frameshift 5′ to the P region, so the amino acid sequence and termination point are different from the other clones despite identical nucleotide sequences. Clone A112 was truncated at the 5′ end. Outside of the pore-forming exon, all three clones are identical at the nucleotide level. Clone B(I) was a construct made for expression studies by using the restriction enzyme *Bsm*FI to cut out pore I from A112 and ligating it into a similarly digested B(II). *B*, Sites of alternative splicing in *Panulirus shaker*. Alternative splicing occurs at the 5′ end, the pore forming region, and the 3′ end. Alternative 5′ exons are not shown. The *boxes* represent exons, whereas the *thin lines between* the *boxes* indicate points of alternative splicing. *C*, Alternative splicing in the pore-forming region of the protein. Three different pore forms were found. The locations of the primers used for RT-PCR to detect these variants in *Panulirus* RNA are shown, with the 3′ primer serving as the RT primer. *D*, Pores I, II, and O were detected from CNS RNA. The products from an RT-PCR-containing CNS RNA and the primers shown in *C* were separated on an 8% acrylamide gel. The template in each PCR is written *above* the lane. *E*, The splice sites and amino acid sequences of the three pore forms. The three pore forms were aligned to the *Drosophila* pore exon, with identical amino acids *boxed*. Indicated *above* the sequence are the positions of the P region amino acids that differ between *Drosophila shaker* B and *Panulirus shaker*.

were obtained by screening. Clones B(II) and B(0) contained complete open reading frames and substantial sequence identity. However, clone B(0) lacked an exon coding for the pore-forming S5–S6 region and was truncated relative to B(II) at the C terminus. Because of the absence of a pore-forming exon, the B(0) reading frame was shifted for residues 3′ to the pore exon splice site, resulting in a premature stop codon 66 amino acids 3′ to the splice site. Clone A112 lacked the amino end of the protein and was substantially identical to the 3′ end of B(II). However, it had an alternative exon at the pore-forming S5–S6 region (Fig. 1*A*).

These results, along with subsequent 5′ rapid amplification of cDNA ends (RACE) reactions for additional 5′ ends, have allowed us to determine the positions of alternative splice sites in *Panulirus shaker* (Fig. 1*B*). Alternative splicing was found at the 5′ end as in *Drosophila*, with eight complete 5′ splice variants detected to date (Kim et al., 1997); only one splice form is shown in Figure 1*B*. There are two invariant regions, one of which extends from the 5′ splice site to the middle of the fifth transmembrane domain, S5, and the other from the end of the P region to near the end of the C terminus. At the 3′ end, a single

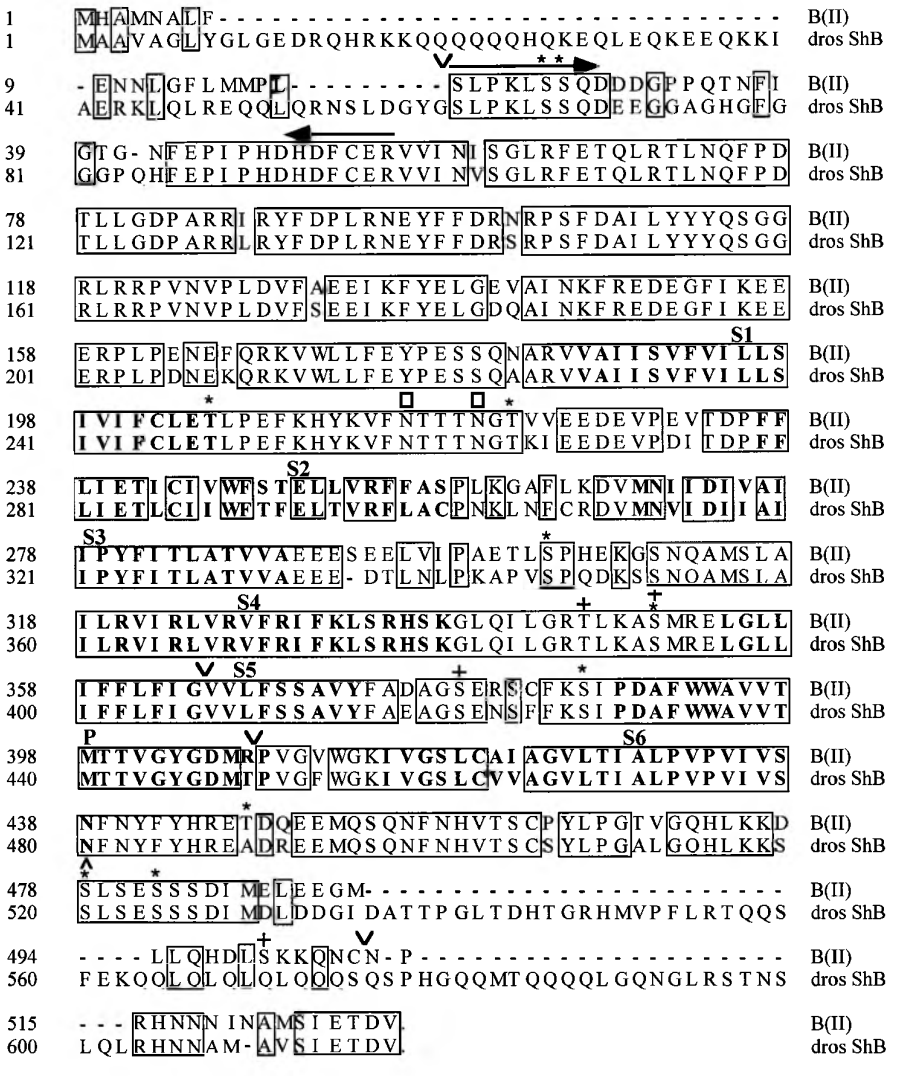

Figure 2. Alignment of the amino acid sequences between B(II) and *Drosophila shaker* B (*dros ShB*). Identical amino acids are *boxed*. Transmembrane-spanning domains S1–S6 and the pore-forming P region are labeled and shown in *bold type*. The sequences are 83% identical at the amino acid level. The locations of the PCR primers used to screen the cDNA libraries are shown as *arrows* near the 5′ end. The known exon boundaries for alternative splicing at the N terminal, P region, and C terminal are marked ∨. Consensus phosphorylation and glycosylation sites are indicated *above* the sequence: PKC (+), casein kinase II (*), and PKA (∧) phosphorylation sites; N-linked glycosylation sites (□). The putative sites between S1 and S2, S3 and S4, and S5 and the P region are thought to be extracellular and would be phosphorylated only by ectoprotein kinases. The lobster *shaker* B(I) and alternate P region exon II nucleotide sequences have been processed by the Genomic Sequence DataBase under accession numbers AF017129 and AF017130.

alternative exon, which we call α, has been found; it was present in five independently isolated splice variants containing a P region exon and was absent in all three independently isolated variants lacking a P region exon. In the pore-forming region of the protein between S5 and S6, three splice variants were found: pore I in clone A112, pore II in B(II), and pore 0 in clone B(0) (Fig. 1*B,C*). Pore exons I and II are 43 amino acids long and very similar to each other, with 75% nucleotide identity. When translated, these exons differ in only four amino acids (Fig. 1*E*). Three of these differences are conservative changes: 376 E (pore I) or D (pore II), 381 K (pore I) or R, and 383 Y (pore I) or C. However, at the 3′ end of the exon, residue 407 is either an uncharged T (pore I) or a positively charged R (pore II). As described in Discussion, this residue is thought to lie at the outer mouth of the pore, and the addition of a positive charge in pore II at this site might explain some of the unique electrophysiological properties of a pore II-containing channel. The third splice variant, pore 0, lacks the entire pore-forming exon. As described above, this creates a frameshift that results in a premature stop codon.

To confirm the presence of these three splice variants in *Panulirus* RNA, we performed an RT-PCR on RNA isolated from combined ganglia (abdominal, cerebral, and thoracic; Fig. 1*D*). The primers used in the PCR span the pore-forming region (Fig. 1*C*), with the 3′ primer serving as an RT primer as well. The products were run on an acrylamide gel (Fig. 1*D*). A band representing both pore-containing exons I and II and a second smaller band representing pore 0 can be seen. The identity of these bands was confirmed by gel-purifying the two sets of bands, subcloning, and sequencing the products.

We believe this to be the first example of alternative splicing in the pore-forming region of a voltage-dependent ion channel. The differences between pore I and pore II are too numerous and varied to be attributable to RNA editing (Powell et al., 1987), with 32 of 129 base pairs differing between these pore-forming exons. These differences could not be attributable to gene duplication, as is seen in mammalian *shaker* genes (Stuhmer et al., 1989; Beckh and Pongs, 1990; Chandy et al., 1990), because the only differences at the nucleotide level in the entire core of the protein were found in the pore-forming exon.

Comparing *Panulirus* and *Drosophila shaker*

There was 83% overall identity at the amino acid level between *Panulirus* and *Drosophila shaker* (Fig. 2). Substantially less homology was seen at the N terminus, where numerous alternative exons were found. In *Drosophila*, there was no significant homology between the alternatively spliced N termini (Kamb et al., 1988; Pongs et al., 1988; Schwarz et al., 1988), and in *Panulirus* the alternative exons did not resemble each

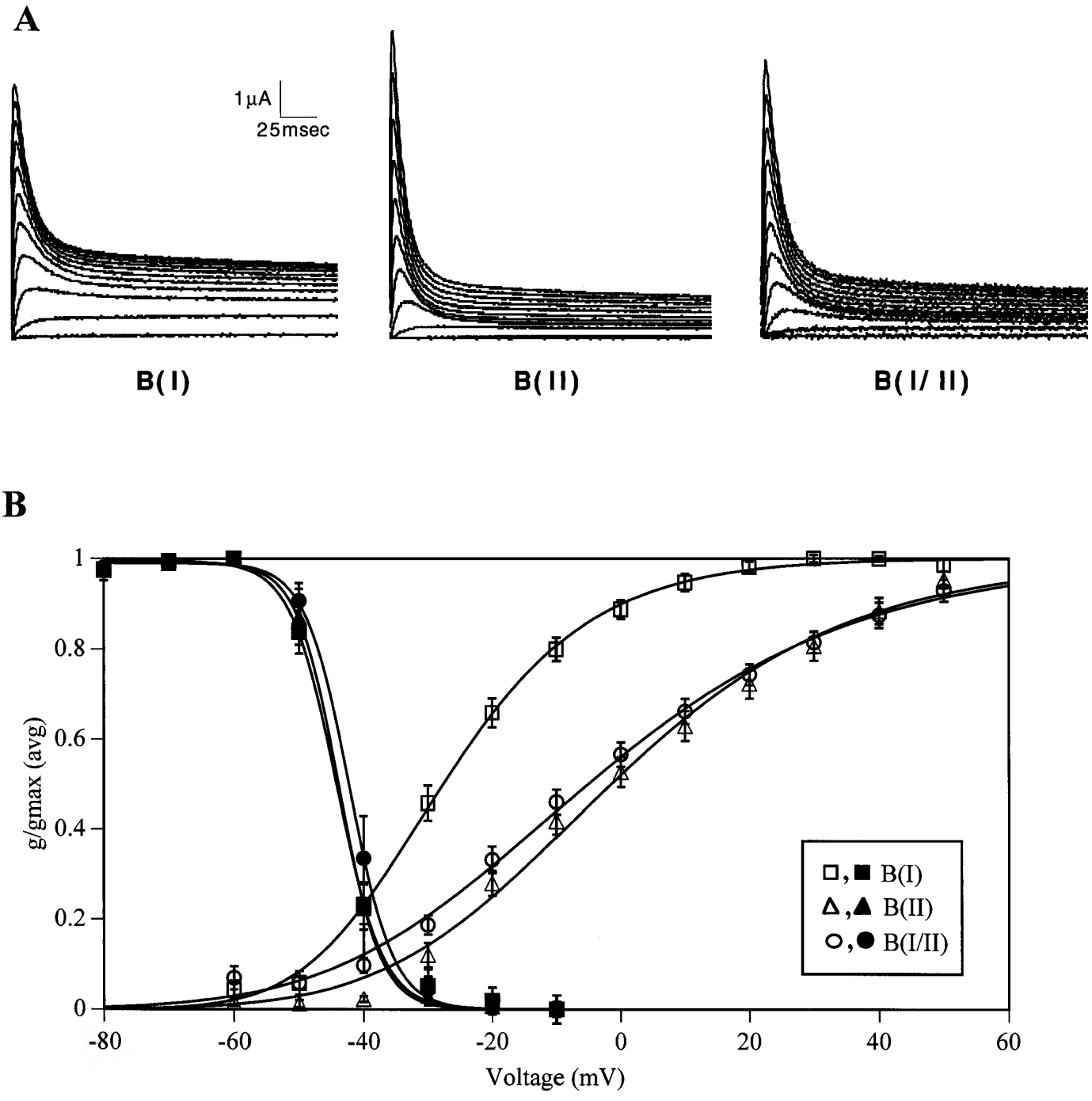

Figure 3. Alternatively spliced channels produce different currents. *A*, Current traces of B(I), B(II), and B(I/II). Electrophysiological studies were performed in *Xenopus* oocytes (see Materials and Methods). The traces were for 10 mV steps from a holding potential of −70 mV to between −60 and +50 mV. *B*, Voltage dependence of activation and inactivation for the different pore forms. The error bars for SEM are shown. The activation curves (*open symbols*) were different for the three forms, whereas the inactivation curves (*filled symbols*) were nearly identical.

other or any of the *Drosophila* exons. There was also low homology at the C terminus, which, in *Panulirus shaker* (with the 3′ α exon), was 52 amino acids shorter than *Drosophila ShB*. However, the last six amino acids were identical. In *Drosophila* the last four amino acids have been shown to be responsible for protein clustering and localization to the nerve terminal (Tejedor et al., 1997). In the P region only one *Drosophila* exon has been isolated from RNA (Baumann et al., 1988; Papazian et al., 1987; Kamb et al., 1988; K. McCormack, 1991). As seen in Figure 1*E*, the *Drosophila* P region is most similar to *Panulirus* pore exon I, differing in only two amino acids. One of these results is an additional positive charge in *Panulirus shaker* (N423 in *Drosophila* vs K381 in *Panulirus*). The *Panulirus* pore exon II differs from the *Drosophila* P region by four amino acids, resulting in the addition of two positive charges (N423 and T449 in *Drosophila* vs R381 and R407 in *Panulirus*).

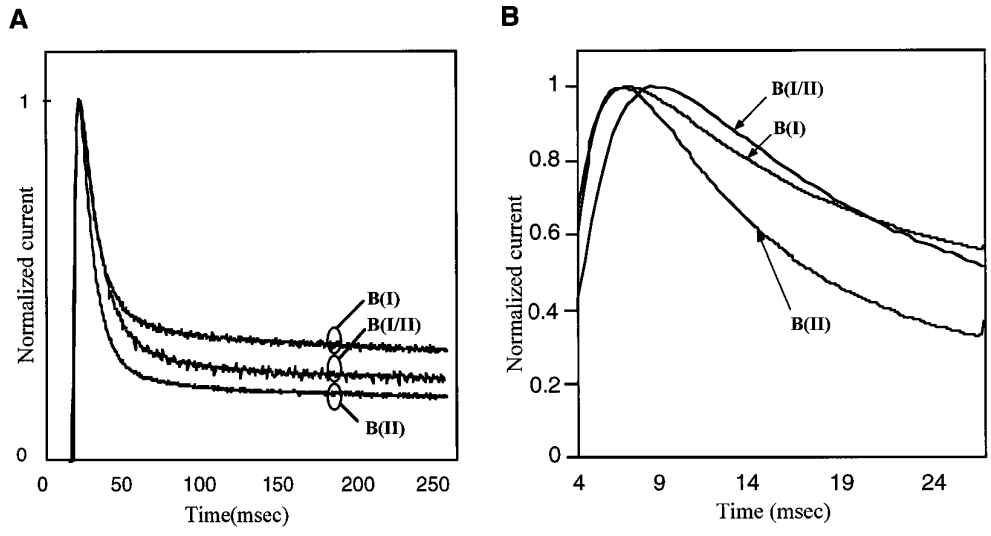

Figure 4. Kinetics of activation and inactivation for the different pore forms. *A*, Differences in the kinetics of inactivation. Current traces were obtained by delivering a 300 msec step from a holding potential of −70 to +20 mV. B(I) and B(II) are homomultimers containing the designated pore. B(I/II) is a mixed population of heteromers and homotetramers. The mixed population of channels displays kinetics of inactivation intermediate between the two homomers. *B*, Differences in the kinetics of activation. B(I) and B(II) have nearly identical kinetics of activation, whereas the I/II heteromer channels activate more slowly.

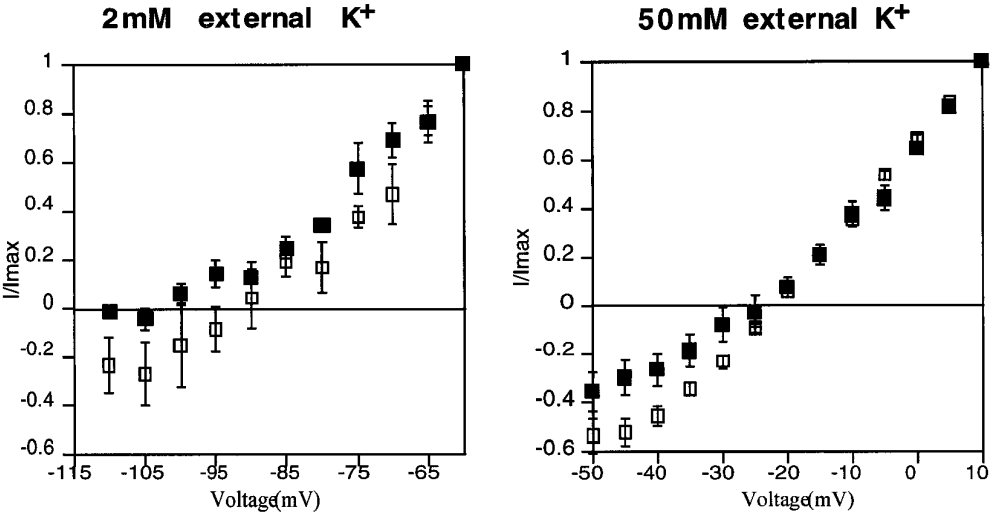

Figure 5. Rectification of tail currents. Outward rectification of current flow measured from tail currents elicited from a step to +20 mV by a series of steps to the indicated voltages. The current amplitudes were normalized by dividing by the maximal current at the most depolarized step. □, B(I); ■, B(II). B(II) shows significant outward rectification in 2 mM external K^+, whereas B(I) shows much less outward rectification. Less outward rectification is observed with increasing external K^+ concentrations.

Potential post-translational modification sites of *shaker* channels

Shaker channels are subject to post-translational modifications, including phosphorylation (Rehm et al., 1989; Moran et al., 1991; Drain et al., 1992; Isacoff et al., 1992; Levitan, 1994; Scott et al., 1994; Holmes et al., 1996) and glycosylation (Rehm et al., 1989; Scott et al., 1990, 1994). As indicated in Figure 2, *Panulirus shaker* contains two putative N-linked glycosylation sites (Hubbard and Ivatt, 1981; Kornfeld and Kornfeld, 1985), four putative protein kinase C phosphorylation sites (Kishimoto et al., 1985; Woodgett et al., 1986), 10 putative casein kinase II phosphorylation sites (Kuenzel et al., 1987; Aitken, 1990), and a single putative cAMP-dependent protein kinase site (Krebs and Beavo, 1979; Aitken, 1990). Many of these, however, are located in regions thought to be extracellular, based on current models of *shaker* protein topology (Durell and Guy, 1992, 1996), and thus would be phosphorylated only by ectoprotein kinases (Merlo et al., 1997).

Electrophysiological characterization of *Panulirus shaker* P region variants

We decided to explore the functional consequences of the three splice variants in the P region of *Panulirus shaker*. To do so, we expressed three clones, which are identical except for the P region, in *Xenopus* oocytes. Clone B(I), containing pore I, was made by using the restriction enzyme *Bsm*FI to cut pore I from the A112 clone and ligate it into a similarly digested B(II). The original B(II) and B(0) clones were used for pore II and pore 0. All three have identical type B 5′ exons, and B(I) and B(II) both have the 3′ α exon. Because of the frameshift resulting from pore 0, clone B(0) terminates before the 3′ α exon is reached. Thus, B(I) and B(II) generate proteins that are identical except for four amino acids in the P region, while B(0) generates a protein that is identical up to the P region splice site and markedly different 3′ to this splice site. We have shown by RT-PCR that transcripts containing the 5′ B exon, together with either pore I or pore II, are present in *Panulirus* neurons (Baro et al., 1996a; R. Harris-Warrick, unpublished data).

RNA was prepared from each clone and expressed by injection into *Xenopus* oocytes. Two-electrode voltage-clamp expression studies of the three pore forms were performed as described previously (Baro et al., 1996b). In our studies of B(I) and B(II), we found that exchanging pore exon I for pore exon II while keeping the rest of the coding sequence identical, produced four significant differences in the characteristics of the two channels.

First, B(I) and B(II) have a markedly different voltage depen-

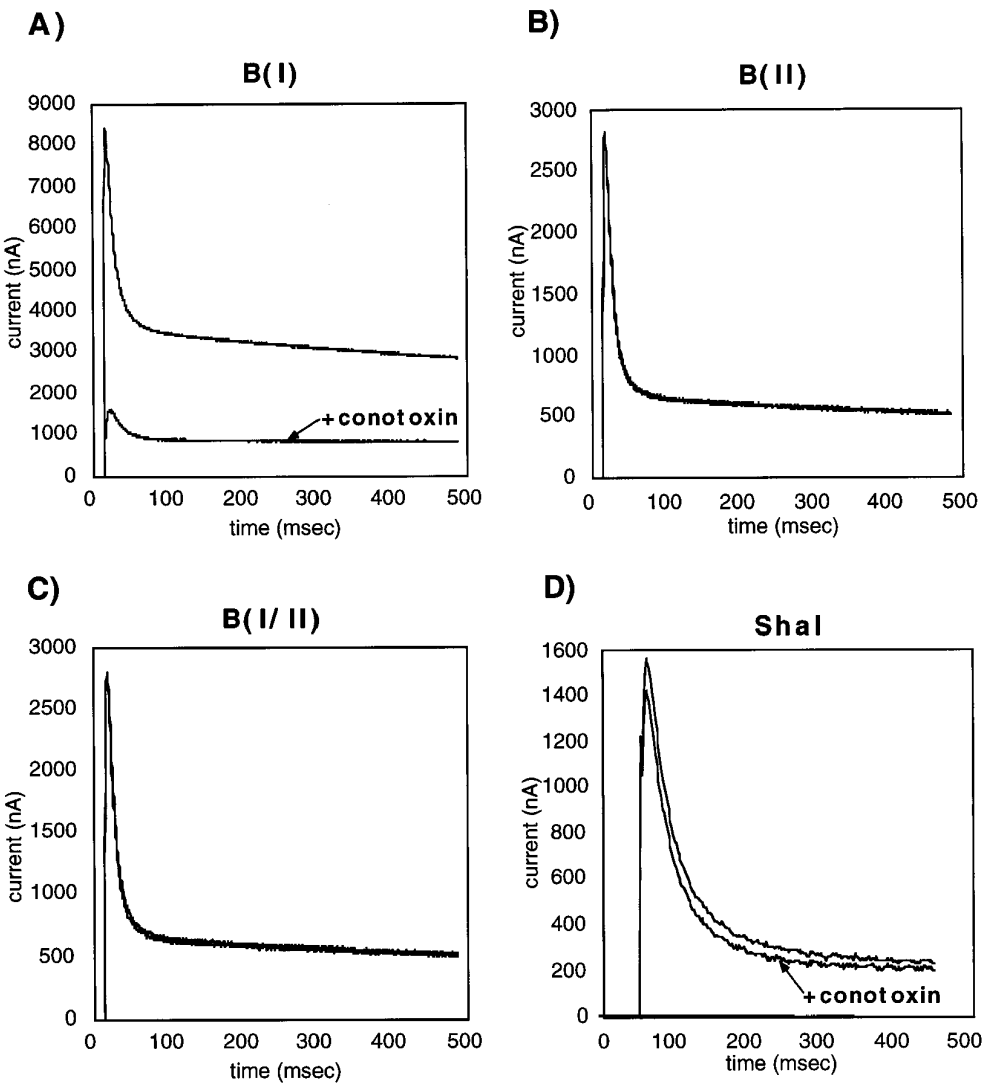

Figure 6. κ-Conotoxin PVIIA selectively blocks one pore form. *A*, κ-Conotoxin PVIIA (1 μM) significantly reduces B(I). *B*, κ-Conotoxin PVIIA does not block B(II). The current traces in control conditions and in the presence of 10 μM κ-conotoxin PVIIA are overlaid. κ-Conotoxin PVIIA (1 μM) also does not block B(I/II) (*C*) or *Panulirus shal* (*D*).

dence of activation (Fig. 3, Table 1). The set of currents evoked from a V_{hold} of −70 to +50 mV in 10 mV steps for the two pore forms is shown in Figure 3. Both clones evoked an outward current with inactivating and noninactivating components. Figure 3*B* shows normalized peak conductance as a function of voltage, with the data fit by a third-order Boltzmann relation. The $V_{1/2act}$ in B(I) was 15 mV more hyperpolarized than B(II), and its g/V relation had a significantly steeper slope (14 mV/*e*-fold) than B(II) (23 mV/*e*-fold) (Table 1). Using the method of limiting slopes (Logothetis et al., 1992), we estimated the gating charge z to be 1.9 for B(I) and 2.7 for B(II). As a consequence of these differences, the current evoked by B(I) was half-maximal at −28 mV, whereas for B(II) one-half of the current was activated at −2 mV. Despite these differences in the voltage dependence of activation, the voltage dependence of inactivation was nearly identical for the two splice forms (Fig. 3, Table 1). The $V_{1/2inact}$ was almost identical, and the slope of the g/V Boltzmann fit was only slightly steeper for pore II.

Second, there were differences in the kinetics of inactivation between the two pore forms (Figs. 3*A*, 4*A*, Table 2). For both splice forms the kinetics of inactivation at +20 mV were best fit as the sum of three exponential components and a significant noninactivating component. For all three components B(I) had slower rates of inactivation than B(II) (Table 2). At +20 mV the fast time constant τ_{fast} was 29% slower in B(I) than in B(II); the intermediate time constant τ_{int} was approximately five times slower, and the slow time constant τ_{slow} was approximately two times slower. In addition to having slower time constants, a smaller fraction of the B(I) current inactivated rapidly, as compared with B(II) (50 vs 75%), and a larger percentage inactivated with τ_{slow} (25 vs 13%). There is a significant fraction of noninactivating current in both pore forms, and this was more than twofold larger in B(I) than in B(II) (Figs. 3*A*, 4*A*, Table 2). The fraction of noninactivating current is largest in B(I) at lower voltage steps; the inactivating component becomes prominent at higher voltage steps (Fig. 3*A*). The fraction of noninactivating current is also larger at lower voltage steps in B(II), although to a lesser degree. Thus, *shaker* channels with pore I showed an overall slower rate of inactivation because of a combination of slower time constants, a smaller fraction of rapidly inactivating current, and a larger fraction of slowly inactivating and noninactivating current relative to pore II. In contrast, the activation rates of the two pore forms appeared to be nearly identical: this was estimated from the the time-to-peak current, which was 6.8 ± 0.2 msec (n = 17) for B(I) and 6.6 ± 0.2 msec (n = 19) for B(II) (Fig. 4*B*, Table 2).

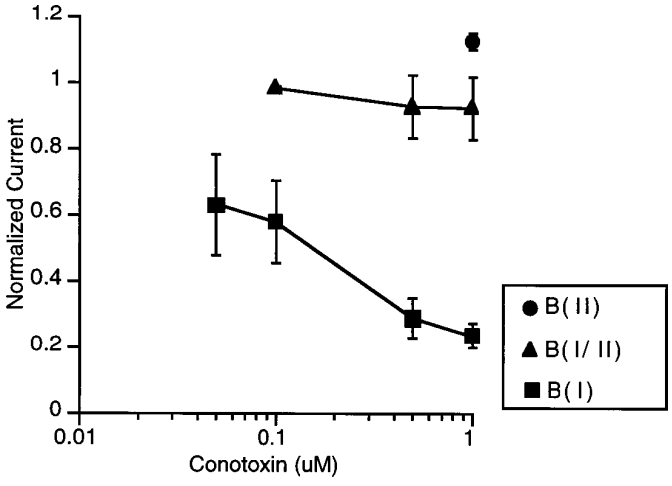

Figure 7. Dose–response curves of B(I), B(II), and B(I/II) to κ-conotoxin PVIIA. ●, B(II); ▲, B(I/II); ■, B(I). The error bars for SEM are shown. B(II) and the heteromer B(I/II) are insensitive to κ-conotoxin PVIIA. The IC_{50} value for B(I) is 142 nM.

Third, differences in drug sensitivity were found between the two forms. 4-Aminopyridine (4-AP) is a classical I_A blocker: B(I) was somewhat more sensitive to 5 mM extracellular 4-AP, showing a 97 ± 1% (n = 3) block, as compared with a 78 ± 4% (n = 6) block for B(II). Similar results were found with 96 mM extracellular tetraethylammonium (TEA^+), which caused a 85 ± 4% (n = 4) block for B(I) but only a 44 ± 9% (n = 6) block for B(II). Thus, the pore I form is more sensitive to these positively charged open channel blockers than pore II channels.

Fourth, measurements of tail currents on repolarization after an activating prestep showed significant differences in current rectification between the two pore forms (Fig. 5). In 2 mM extracellular K^+, both pore forms carried similar outward currents, but B(II) showed significant outward rectification and essentially was unable to carry an inward K^+ current below E_K. In contrast, B(I) showed much less outward rectification and could carry a robust inward current below E_K. With elevated extracellular K^+ (10 and 50 mM K^+), both pore forms could carry an inward K^+ current, but pore I continued to carry greater inward current at voltages below E_K (Fig. 5).

Measuring from the reversal potentials of the tail currents, the potassium selectivity was not altered between the two splice forms: the slope of V_{rev} versus extracellular K^+ was 52.1 mV per 10-fold change in external K^+ for B(I) and 51.7 mV for B(II). In normal ND96 (2 mM K^+), V_{rev} was −97.4 ± 2.6 mV for B(I) and −100.6 ± 1.5 mV for B(II), although this value was difficult to measure because of the extreme rectification of B(II).

As might be expected, RNA from clone B(0) (pore 0) did not produce a functional voltage-activated or leak channel when injected into *Xenopus* oocytes. It also did not function as a dominant negative for B(II): when coinjected at a 1:1 ratio with B(II) RNA, B(0) did not alter the maximal current or any of the electrophysiological properties of B(II) (data not shown).

Heteromers between pore forms I and II

Voltage-clamp studies were performed on heteromers formed when B(I) and B(II) RNAs were coinjected in a 1:1 ratio. We believe heteromers are formed between the two splice forms, because the four amino acid differences are not in the NAB region responsible for potassium channel assembly (Xu et al., 1995). The resulting currents had electrophysiological characteristics intermediate between the homomers for most parameters tested (Figs. 3, 4, Tables 1, 2).

The $V_{1/2act}$ (−39.6 ± 0.9 mV) for the I/II mixture was intermediate between B(I) and B(II) and was statistically different for all three forms. The $slope_{act}$ for B(I/II) was less steep (25.7 mV/e-fold) than either of the homomer values and was again significantly different from both B(I) and B(II). In contrast to these marked differences in activation voltage dependence, the $V_{1/2inact}$ values were very similar for all three forms although the B(I/II) heteromer was depolarized somewhat from the two homomultimers. The $slope_{inact}$ values for the B(I/II) mixture were again intermediate but not significantly different from B(I).

Table 2 and Figure 4 show the kinetics of activation and inactivation at +20 mV for the B(I/II) mixture, as compared with B(I) and B(II) homomultimers. Interestingly, the activation rate, estimated from the time-to-peak current, was significantly slower (8.7 ± 0.4 msec) for the I/II mixture than for either of the homomultimers, which had statistically identical times to peak (6.8 ± 0.2 and 6.6 ± 0.2 msec for pores I and II). This supports our hypothesis that heteromultimers between pore I and II proteins are formed when mixtures are injected into oocytes. For the kinetics of inactivation, the B(I/II) currents had intermediate values between the homomultimers for all of the parameters (Table 2). Student's t tests showed that these intermediate values were statistically different from both pores I and II for τ_{int}, τ_{slow}, and the percentage of current inactivating with τ_{fast}. For the other parameters the B(I/II) mixture values were lower than but not significantly different from B(I), and both were different from B(II). In conclusion, the B(I/II) currents tended to have voltage and kinetic parameters intermediate between the two homomultimers, but this was not always seen.

Effect of κ-conotoxin PVIIA on *Panulirus* pore variants

We tested the sensitivity of B(I), B(II), and B(I/II) channels to the recently identified potassium channel blocker κ-conotoxin PVIIA from the marine snail *Conus purpurascens* (Terlau et al., 1996). The toxin previously was found to selectively block *Drosophila shaker*, but not two mammalian *shaker* channels, KV1.1 and KV1.4.

The toxin selectively and reversibly blocked B(I) (Fig. 6), with a calculated IC_{50} of 142 nM for B(I) (Fig. 7), as compared with 60–70 nM for *Drosophila shaker* (Terlau et al., 1996). In contrast, the toxin did not block B(II) at all (Figs. 6, 7), even at a concentration of 10 μM. The normalized current value for B(II) in the presence of 1 μM conotoxin was slightly larger than 1, probably because of the sealing of the membrane around the electrodes and improved clamping with time. The toxin had only a marginal effect on mixed B(I/II) currents (Figs. 6, 7), even at concentrations as high as 3 μM. This small block was not statistically significant ($p > 0.05$), but it might be attributable to blockade of B(I) homomers (see Discussion). This result strongly suggests that heteromers between pore I and pore II are formed when B(I) and B(II) RNAs are coinjected. If only homomers were formed with the coinjection studies, significant block of the pore I homomers would have been observed with 1:1 mixtures. The toxin also did not significantly block *Panulirus shal* channels (Fig. 7). Thus κ-conotoxin PVIIA is able to selectively block one pore form of *Panulirus shaker*, but not the other form, heteromers between the two forms, or *Panulirus shal* currents.

We used κ-conotoxin PVIIA to assess the role of the different pore splice forms in *Panulirus* neurons from the stomatogastric

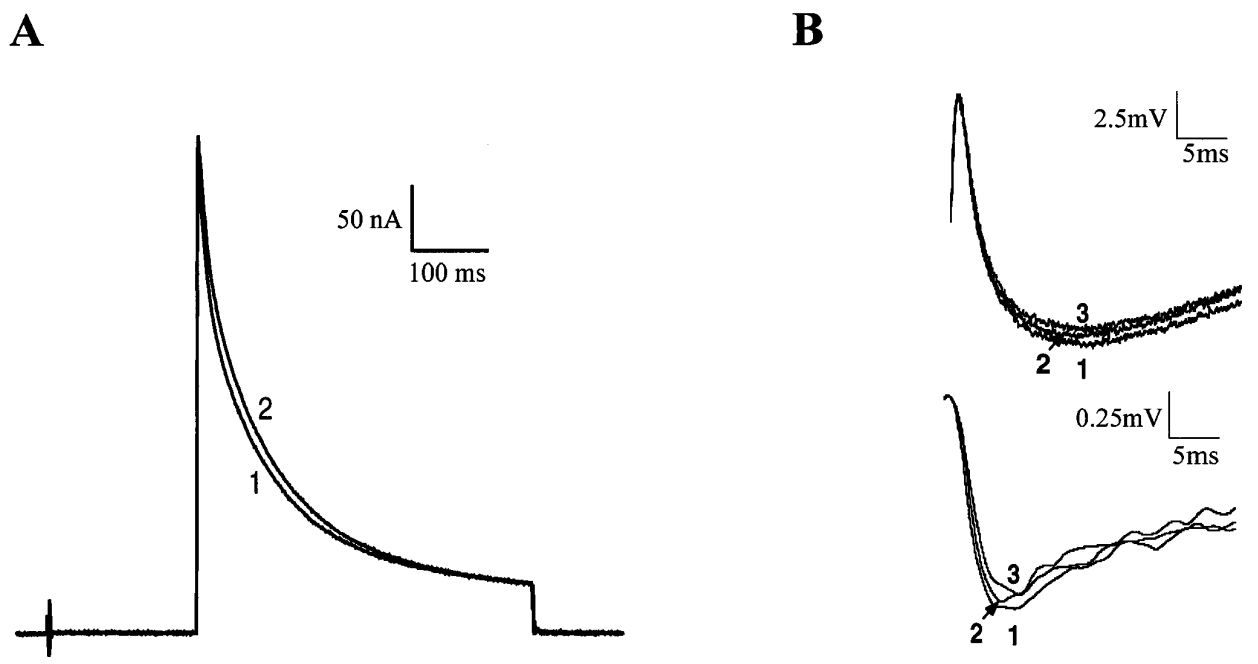

Figure 8. Lack of effects of κ-conotoxin PVIIA on *Panulirus* neurons. *A*, The effect of κ-conotoxin PVIIA on the somatic I_A. The two somatic I_A traces were obtained from a voltage-clamped *Panulirus* pyloric dilator (PD) neuron after 0 min (*trace 1*) or 30 min (*trace 2*) in 2 μM κ-conotoxin PVIIA. The slight increase in I_A could be washed out. *B*, The effect of κ-conotoxin PVIIA on LP/PD synaptic transmission. The *top traces* are the action potentials in the lateral pyloric (LP) neuron, and the *bottom traces* are the corresponding IPSPs of the PD neuron. The traces shows the effects of the toxin before (*trace 1*), in the presence of conotoxin (*trace 2*), and after wash (*trace 3*).

ganglion. We examined the effects of the conotoxin on the somatic I_A in *Panulirus* stomatogastric neurons, using two-electrode voltage clamp. After 30 min, 2 μM κ-conotoxin PVIIA either had no effect on the somatic I_A or caused a slight increase that could be washed out (Fig. 8*A*). This suggests that pore I homomers do not contribute to the somatic I_A in these neurons. We also tested whether the conotoxin could block A-channels involved in the control of synaptic transmission, looking at the spike-evoked inhibitory transmitter release from the lateral pyloric (LP) to the pyloric dilator (PD) neuron. The LP spike-triggered IPSP was signal-averaged under control conditions and in the presence of 1 μM κ-conotoxin PVIIA. The toxin had no reversible effect on this IPSP (Fig. 8*B*).

DISCUSSION

Comparison between pore forms I and II

B(I) and B(II) differ by only four of their 515 amino acids, with three of the changes occurring in the extracellular loop connecting S5 to the P region and the fourth occurring at the 3′ end of the P region (Gross and MacKinnon, 1996) (see Fig. 1). Three of the four substitutions are conservative, whereas the fourth (position 407) adds a positively charged residue (arginine) in B(II). However, these four substitutions alter the voltage dependence of activation, kinetics of inactivation, drug sensitivity, and current rectification of the channels in marked ways. The P region is postulated to form a loop structure that extends toward the central pore region, with the selectivity filter formed by the loops of the four subunits (MacKinnon, 1995; Gross and MacKinnon, 1996; Ranganathan et al., 1996). Extensive site-directed mutagenesis studies have been performed in the pore-forming region of *Drosophila shaker* to determine which residues are critical to channel function (MacKinnon and Miller, 1989; MacKinnon and Yellen, 1990; Hartmann et al., 1991; Yellen et al., 1991; Yool and Schwarz, 1991; Heginbotham and MacKinnon, 1992). On the basis of these earlier results, it appears that many of the biophysical differences we observed between the pore I and II forms of *Panulirus shaker* arise from the addition of the positive charge at residue 407, which is threonine in pore I and positively charged arginine in pore II. This residue is homologous to T449 in *Drosophila shaker* B, which is thought to be the last amino acid in the P region, and has been studied extensively in structure–function analyses (Yool and Schwarz, 1991; Durell and Guy, 1992; Kirsch et al., 1992; Lopez-Barneo et al., 1993).

In *Drosophila shaker*, site-directed mutagenesis of T449 to positively charged lysine or arginine residues has been studied primarily in clones with a Δ6–46 deletion to remove N-type inactivation (Zagotta et al., 1990). Three major effects of adding a positive charge at the outer lip of the channel pore have been reported. First, the addition of a positive charge at 449, T449K, dramatically increased the rate of slow C-type inactivation by 100-fold in the Δ6–46 mutant (Lopez-Barneo et al., 1993). We have found a similar, although much less dramatic, increase in the inactivation rate between pore I (T407) and pore II (R407), with time constants between 40 and 475% faster in pore II (see Fig. 4, Table 2). However, N-type inactivation is still present in B(I) and B(II), as seen by the very rapid initial inactivation in both pore forms (see Fig. 4). This very rapid inactivation is lost when the 5′ B exon is substituted by a shorter 5′ exon (Kim et al., 1997). Second, the T449R mutation caused the *Drosophila* channel to become less sensitive to TEA (MacKinnon and Yellen, 1990; Kavanaugh et el., 1991): the IC_{50} shifted from 17 to >150 mM, which would result in a change from 78 to 39% or less block in 96 mM TEA. This corresponds well to the 85 and 44% blocks we observed with 96 mM TEA in the *Panulirus* pore I (T407) and pore II (R407) variants. Third, in *Drosophila* the R449 variant showed marked outward rectification and carried significantly less

inward K^+ current below E_K than the wild-type T449; this was thought to arise from the addition of a ring of four positive charges at the lip of the pore repelling K^+ entry. In *Panulirus*, an even greater rectification was observed, with no detectable inward current below E_K in pore II (R407) in normal K^+ saline. This stronger effect might result from the additional positive charge at position 381 (R or K in *Panulirus*, equivalent to N423 in *Drosophila*), which might form an additional barrier to K^+ entry from the exterior. N423 is modeled to be in the extracellular domain connecting S5 and the P region at a distance from the hairpin loop (Durell and Guy, 1992, 1996), but its function has not been analyzed in structure–function studies. In conclusion, a charged arginine residue at position 407 may explain three of the four unique properties of *Panulirus* pore II channels, as compared with threonine-containing pore I channels.

We report the novel finding that pore I- and pore II-containing channels showed a markedly different voltage dependence of activation, with a 15 mV shift in $V_{1/2act}$ and a significant difference in the slope of the g/V relation; these results suggest that the voltage- dependence and gating charge for opening the channel are affected by amino acid substitutions in the S5–P region. In *Drosophila shaker*, the voltage dependence of activation was altered by mutations in the voltage-sensing S4 transmembrane-spanning domain (Stuhmer et al., 1989, 1991; Benzanilla et al., 1991; Liman et al., 1991; McCormack et al., 1991; Papazian et al., 1991; Logothetis et al., 1992; Pardo et al., 1992), S2 (Planells-Cases et al., 1995), the leucine zipper region between S4 and S5 (McCormack et al., 1991), and by changing the N terminus with different splice variants (Stocker et al., 1990). However, *Panulirus* B(I) and B(II) are identical in these regions. Thus, amino acids in or adjacent to the P region must interact with S4 and/or other regions of the protein to determine the stability of the closed versus open states and the gating current. Pores I and II differ in charge only at position 407 (T vs R), but charge-conserving substitutions also could alter voltage sensitivity; charge-conserving mutations in the S4 domain were shown to alter voltage dependence in other channels (Lopez et al., 1991). In addition, although the pore I to II substitution clearly altered the voltage dependence of activation, the voltage dependence of inactivation was not affected significantly. In *Drosophila* and several mammalian transient *Shaker* family channels, voltage-dependent activation and inactivation are thought to be coupled (Zagotta and Aldrich, 1990; Bertoli et al., 1994), but our data do not provide evidence for such coupling in *Panulirus shaker*.

Heteromers between pore I and pore II subunits

Heteromers between potassium channel proteins within the *shaker* subfamily were shown to be produced by coinjection studies in *Xenopus* oocytes (Isacoff et al., 1990; McCormack et al., 1990; Ruppersberg et al., 1990; MacKinnon, 1991) as well as *in vivo* (Sheng et al., 1993; Wang et al., 1993). A region near the N terminal (called the NAB region) 5′ to the S1 transmembrane-spanning domain is responsible for subunit assembly (Li et al., 1992; Shen et al., 1993; Xu et al., 1995). This region is conserved among *Drosophila*, mammals, and *Panulirus*, and therefore heteromeric channel formation between proteins with different P regions is to be expected when coinjection studies of different splice variants are performed (Xu et al., 1995). When we coinjected B(I) and B(II), the resulting currents displayed electrophysiological characteristics that were primarily intermediate between the two pore forms (see Figs. 3, 4, Tables 1, 2). Two results support our hypothesis that heteromers were formed in these coinjection studies. First, the B(I/II) currents had a slower activation rate than either B(I) or B(II) alone (see Fig. 4, Table 2). Second, as described below, B(I) is sensitive to κ-conotoxin PVIIA, whereas B(II) is completely resistant, and the B(I/II) currents are >90% resistant (see Figs. 6, 7). If only B(I) and B(II) homomers were present after coinjection of both RNAs, we would expect a significant reduction in current with the toxin, which was not seen. The B(I/II) currents had a $slope_{act}$, which was less steep than either homomer. This could have two explanations. First, on coinjection of pore I and pore II RNAs, all tetrameric combinations are formed, with a binomial distribution, from B(I) homotetramers through all possible heteromers (1:3; 2:2; 3:1) to B(II) homotetramers. The different channels may have a different voltage dependence, resulting in a smeared distribution and thus a lower slope of the V activation curve. A second possibility is that the heteromer channels are less sensitive to a depolarizing pulse, possibly because of an asymmetrical charge alignment.

Pore-selective block by κ-conotoxin PVIIA

The potassium channel blocker κ-conotoxin PVIIA recently was identified from *Conus purpurascens* (Terlau et al., 1996). This toxin was found to block *Drosophila shaker* channels, but not the mammalian *shaker* channels KV1.1 and KV1.4. We found that this toxin shows exquisite selectivity for *Panulirus* pore I homomultimers. It blocked B(I) currents with an IC_{50} of 142 nM, but it had no detectable effect on B(II) currents even at 10 μM (see Fig. 7). In addition, the conotoxin did not significantly block currents generated from the related transient K^+ current gene, *shal* (see Fig. 7). At 1 μM it evoked an average 8% decrease in peak currents generated by 1:1 mixtures of B(I) and B(II) RNA. This is similar to the 6.25% of channels predicted by a binomial distribution to be homomeric B(I) channels if we assume that (1) B(I) and B(II) are expressed equally in oocytes and that (2) B(I) and B(II) proteins assemble randomly into tetramers with one another. Thus, our data support the hypothesis that a heterotetramer with at least one pore II-containing subunit will be completely resistant to κ-conotoxin PVIIA. κ-conotoxin PVIIA is a 27 amino acid peptide with six positively charged residues. By having one or more positively charged arginines at residue 407 in the P region, channel tetramers with at least one B(II) subunit are insensitive to the toxin, presumably by repulsion of the positively charged toxin.

When the toxin was applied to stomatogastric ganglion (STG) neurons in *Panulirus*, it was found to have no effect on synaptic transmission. *Shaker* pore I and pore II forms are both expressed in STG neurons (Baro et al., 1996a; R. Harris-Warrick, unpublished data), so it is likely that they form heteromers that are resistant to the toxin. We cannot determine what role these heteromers might play in control of synaptic transmission. The only conclusion we can draw from this result is that B(I) homotetramers do not play a major role in synaptic transmission. The transient K^+ current measured in STG neuronal cell bodies also was unaffected by the toxin. Again, our only conclusion is that the *shaker* pore I homomers do not contribute to this current. We have presented evidence elsewhere (Baro et al., 1997) suggesting that the somatic I_A in STG neurons is encoded mainly by *shal* rather than *shaker*, and the resistance of I_A to κ-conotoxin PVIIA provides support for this hypothesis.

Although the pore 0 isoform, lacking an S5–P region exon altogether, represents a clearly measurable fraction of the total *shaker* RNA (see Fig. 1*D*), it does not express a voltage-activated

channel and apparently cannot interact with pore-containing *shaker* proteins in the *Xenopus* oocyte expression system. We do not know the possible function of this isoform: it simply may arise from an error in RNA splicing or may be an unusual way of downregulating channel expression. Because the NAB region is totally preserved in B(0), it would be theoretically possible for heteromers to be formed with other *shaker* subunits, based purely on its protein sequence. Since B(0) had no effect in coinjection studies with B(II), pore 0-containing subunits might be degraded in the endoplasmic reticulum due to improper protein folding with the frameshift after the P region (Hurtley and Helenius, 1989). Alternatively, the shift in reading frame 3′ to the missing pore exon might produce a protein whose structure is too disrupted to interact with other *shaker* proteins.

In conclusion, we have found novel alternative splicing in the pore-forming region of *Panulirus shaker*. By merely changing four amino acids in the entire protein, channels with very different biophysical characteristics and drug sensitivity are created naturally. One can see how this alternative splicing mechanism can be used to precisely regulate channel function at a molecular level.

REFERENCES

Aitken A (1990) Identification of protein consensus sequences: active site and DNA-binding motifs, phosphorylation, and other post-translational modifications. New York: Ellis Horwood.

Baro DJ, Cole CL, Zarrin AR, Hughes S, Harris-Warrick RM (1994) *Shab* gene expression in identified neurons of the pyloric network in the lobster stomatogastric ganglion. Receptors Channels 2:193–205.

Baro DJ, Cole CL, Harris-Warrick RM (1996a) RT-PCR analysis of *shaker*, *shab*, *shaw*, and *shal* gene expression in single neurons and glial cells. Receptors Channels 4:149–159.

Baro DJ, Coniglio L, Cole CL, Rodriguez H, Lubell J, Kim M, Harris-Warrick RM (1996b) Lobster *shal*: comparison with *Drosophila shal* and native potassium currents in identified neurons. J Neurosci 16:1689–1701.

Baro DJ, Levini RM, Kim MT, Willms AR, Lanning CC, Rodriguez HE, Harris-Warrick RM (1997) Quantitative single-cell RT-PCR demonstrates that A-current magnitude varies as a linear function of *shal* gene expression in identified stomatogastric neurons. J Neurosci 17:6597–6610.

Baumann A, Grupe A, Ackerman A, Pongs O (1988) Structure of the voltage-dependent potassium channel is highly conserved from *Drosophila* to vertebrate central nervous systems. EMBO J 7:2457–2463.

Beckh S, Pongs O (1990) Members of the RCK potassium family are differentially expressed in the rat nervous system. EMBO J 9:777–782.

Benzanilla F, Perozo E, Papazian DM, Stefani E (1991) Molecular basis of gating charge immobilization in *Shaker* potassium channels. Science 254:679–683.

Bertoli A, Moran O, Conti F (1994) Activation and deactivation properties of rat brain K^+ channels of the *Shaker*-related subfamily. Eur Biophys J 23:379–384.

Chandy KG, Williams CB, Spencer RH, Aguilar BA, Ghanshani S, Tempel B, Gutman GA (1990) A family of three mouse potassium channel genes with intronless coding regions. Science 247:973–975.

Drain PF, McEachern AE, Aldrich RW (1992) Modulation of *Shaker* potassium channel inactivation gating by phosphatase and protein kinase. Biophys J 61:A13.

Durell SR, Guy HR (1992) Atomic scale structure and functional models of voltage-gated potassium channels. Biophys J 62:238–250.

Durell SR, Guy HR (1996) Structural model of the outer vestibule and selectivity filter of the *Shaker* voltage-gated K^+ channel. Neuropharmacology 35:761–773.

Furakawa Y, Kandel E, Pfaffinger P (1992) Three types of early transient potassium currents in *Aplysia* neurons. J Neurosci 12:989–1000.

Gross A, MacKinnon R (1996) Agitoxin footprinting the *shaker* potassium channel pore. Neuron 16:399–406.

Harris-Warrick RM, Coniglio LM, Barazangi N, Guckenheimer J, Gueron S (1995) Dopamine modulation of transient potassium current evokes phase shifts in a central pattern generator network. J Neurosci 15:342–358.

Hartmann HA, Kirsch GE, Drewe JA, Taglialatela M, Joho RH, Brown AM (1991) Exchange of conduction pathways between two related K^+ channels. Science 251:942–944.

Heginbotham L, MacKinnon R (1992) The aromatic binding site for tetraethylammonium ion on potassium channels. Neuron 8:483–491.

Hille B (1992) Ionic channels of excitable membranes, 2nd Ed. Sunderland, MA: Sinauer.

Holmes TC, Fadool DA, Levitan IB (1996) Tyrosine phosphorylation of the KV1.3 potassium channel. J Neurosci 16:1581–1590.

Hubbard CS, Ivatt RJ (1981) Synthesis and processing of asparagine-linked oligosaccharides. Annu Rev Biochem 50:555–583.

Hurtley SM, Helenius A (1989) Protein oligomerization in the endoplasmic reticulum. Annu Rev Cell Biol 5:277–308.

Isacoff EY, Jan YN, Jan LY (1990) Evidence for the formation of heteromultimeric potassium channels in *Xenopus* oocytes. Nature 345:531–534.

Isacoff EY, Kimmerly W, Jan YN, Jan LY (1992) Phosphorylation and modulation of the *Shaker* potassium channel by protein kinase C. Biophys J 61:A13.

Iverson LE, Tanouye MA, Lester HA, Davidson N, Rudy B (1988) A-type potassium channels expressed from *Shaker* locus cDNA. Proc Natl Acad Sci USA 85:5723–5727.

Johnson BR, Peck JH, Harris-Warrick RM (1995) Distributed amine modulation of graded chemical transmission in the pyloric network of the lobster stomatogastric ganglion. J Neurophysiol 74:437–452.

Kamb A, Tseng-Crank J, Tanouye MA (1988) Multiple products of the *Shaker* gene may contribute to potassium channel diversity. Neuron 1:421–430.

Kavanaugh MP, Osborne PO, Varnum M, Busch AE, Adelman JP, North RA (1991) Interaction between tetraethylammonium and amino acid residues in the pore of rat cloned voltage-dependent potassium channels. J Biol Chem 266:7583–7587.

Kim M, Baro DJ, Lanning CC, Doshi M, Moskowitz H, Farnham J, Harris-Warrick R (1997) Expression of *Panulirus shaker* potassium channel splice variants. Receptors Channels, in press.

Kirsch GE, Drewe JA, Hartmann HA, Taglialatela M, DeBiasi M, Brown AM, Joho RH (1992) Differences between the deep pores of K^+ channels determined by an interacting pair of nonpolar amino acids. Neuron 8:499–505.

Kishimoto A, Nishiyama K, Nakanishi H, Uratsuji Y, Nomura H, Takeyama Y, Nishizuka Y (1985) Studies on the phosphorylation of myelin basic protein by protein kinase C and adenosine 3′:5′-monophosphate-dependent protein kinase. J Biol Chem 260:12492–12499.

Kornfeld R, Kornfeld S (1985) Assembly of asparagine-linked oligosaccharides. Annu Rev Biochem 54:631–664.

Krebs EG, Beavo JA (1979) Phosphorylation–dephosphorylation of enzymes. Annu Rev Biochem 48:923–959.

Kuenzel EA, Mulligan JA, Sommercorn J, Krebs EG (1987) Substrate specificity determinants for casein kinase II as deduced from studies with synthetic peptides. J Biol Chem 262:9136–9140.

Levitan IB (1994) Modulation of ion channels by protein phosphorylation and dephosphorylation. Annu Rev Physiol 56:193–212.

Li M, Jan YN, Jan LY (1992) Specification of subunit assembly by the hydrophilic amino-terminal domain of the *Shaker* potassium channel. Science 257:1225–1230.

Liman ER, Hess P, Weaver F, Koren G (1991) Voltage-sensing residues in the S4 region of a mammalian K^+ channel. Nature 353:752–756.

Logothetis DE, Movahedi S, Satler C, Lindpainter K, Nadal-Ginard B (1992) Incremental reductions of positive charge within the S4 region of a voltage-gated K^+ channel result in corresponding decreases in gating charge. Neuron 8:531–540.

Lopez GA, Jan YN, Jan LY (1991) Hydrophobic substitution mutations in the S4 sequence alter voltage-dependent gating in *shaker* K^+ channels. Neuron 7:327–336.

Lopez-Barneo J, Hoshi T, Heinemann S, Aldrich R (1993) Effects of external cations and mutations in the pore region on C-type inactivation of *shaker* potassium channels. Receptors Channels 1:61–71.

MacKinnon R (1991) Determination of the subunit stoichiometry of a voltage-activated potassium channel. Nature 350:232–235.

MacKinnon R (1995) Pore loops: an emerging theme in ion channel structure. Neuron 14:889–892.

MacKinnon R, Miller C (1989) Mutant potassium channels with altered binding of charybdotoxin, a pore-blocking peptide inhibitor. Science 245:1382–1385.

MacKinnon R, Yellen G (1990) Mutations affecting TEA blockade and ion permeation in voltage-activated K^+ channels. Science 250:276–279.
MacKinnon R, Reinhart PH, White MM (1988) Charybdotoxin block of *Shaker* channels suggests that different types of K^+ channels share common structural features. Neuron 1:997–1001.
McCormack K (1991) Structure-function studies of *Drosophila shaker* K^+ channels. PhD thesis, California Institute of Technology.
McCormack T, Vega-Sandez De Miera EC, Rudy B (1990) Molecular cloning of a member of a third class of *Shaker* family K^+ channel genes in mammals. Proc Natl Acad Sci USA 87:5227–5231.
McCormack K, Tanouye MA, Iverson LE, Lin JW, Tamaswami M, McCormack T, Pampanelle JT, Mathew MK, Rudy B (1991) A role for hydrophobic residues in the voltage-dependent gating of *Shaker* K^+ channels. Proc Natl Acad Sci USA 88:2931–2935.
Merlo D, Anelli R, Calissano P, Ciotti MT, Volonte C (1997) Characterization of an ecto-phosphorylated protein of cultured cerebellar granule neurons. J Neurosci Res 47:500–508.
Moran O, Dascal N, Lotan I (1991) Modulation of a *Shaker* potassium A-channel by protein kinase C activation. FEBS Lett 279:256–260.
Papazian DM, Schwarz TL, Tempel BL, Jan YN, Jan LY (1987) Cloning of genomic and complementary DNA for *Shaker*, a putative potassium channel gene from *Drosophila*. Science 237:749–753.
Papazian DM, Timpe LC, Jan YN, Jan LY (1991) Alterations of voltage dependence of *Shaker* potassium channel by mutations in the S4 sequence. Nature 349:305–310.
Pardo LA, Heinemann SH, Terlau H, Ludewig U, Lorra C, Pongs O, Stuhmer W (1992) Extracellular K^+ specifically modulates a rat brain potassium channel. Proc Natl Acad Sci USA 89:2466–2470.
Pfaffinger PJ, Furakawa Y, Zhao B, Dugan D, Kandel E (1991) Cloning and expression of an *Aplysia* K^+ channel and comparison with native *Aplysia* K^+ currents. J Neurosci 11:918–927.
Planells-Cases R, Ferrer-Montiel AV, Patten CD, Montal M (1995) Mutation of conserved negatively charged residues in the S2 and S3 transmembrane segments of a mammalian K^+ channel selectively modulates channel gating. Proc Natl Acad Sci USA 92:9422–9426.
Pongs O, Kecskemethy N, Muller R, Krah-Jentgens I, Baumann A, Kiltz HH, Canal I, Llamazares S, Ferrus A (1988) *Shaker* encodes a family of putative potassium channel proteins in the nervous system of *Drosophila*. EMBO J 7:1087–1096.
Powell LM, Wallis SC, Pease RJ, Edwards YH, Knott TJ, Scott J (1987) A novel form of tissue-specific RNA processing produces apolipoprotein-B48 in intestine. Cell 50:831–840.
Ranganathan R, Lewis JH, MacKinnon R (1996) Spatial localization of the K^+ channel selectivity filter by mutant cycle-based structure analysis. Neuron 16:131–139.
Rehm H, Pelzer S, Cochet C, Chambaz E, Tempel BL, Trautwein W, Pelzer D, Lazdunski M (1989) Dendrotoxin-binding brain membrane protein displays a potassium channel activity that is stimulated by both cAMP-dependent and endogenous phosphorylations. Biochemistry 28:6455–6460.
Ruppersberg JP, Schroter KH, Sakmann B, Stocker M, Sewing S, Pongs O (1990) Heteromultimeric channels formed by rat brain potassium channel proteins. Nature 345:535–537.
Sambrook J, Fritsch EF, Maniatis T (1989) Molecular cloning: a laboratory manual, 2nd Ed. Cold Spring Harbor, NY: Cold Spring Harbor Laboratory.
Schwarz TM, Tempel BL, Papazian DM, Jan YN, Jan LY (1988) Multiple potassium channel components are produced by alternative splicing at the *Shaker* locus in *Drosophila*. Nature 331:137–142.
Scott VES, Parcej DN, Keen JN, Findlay JBC, Dolly JO (1990) Alpha dendrotoxin acceptor from bovine brain is a potassium ion channel protein. J Biol Chem 265:20094–20097.
Scott VES, Muniz ZM, Sewing S, Lichtinghagen R, Parcej DN, Pongs O, Dolly JO (1994) Antibodies specific for distinct KV subunits unveil a hetero-oligomeric basis for subtypes of alpha-dendrotoxin-sensitive K^+ channels in bovine brain. Biochemistry 33:1617–1623.
Serrano EE, Getting PA (1989) Diversity of the transient outward potassium current in somata of identified molluscan neurons. J Neurosci 9:4021–4032.
Shen NV, Chen XH, Boyer MM, Pfaffinger PJ (1993) Deletion analysis of K^+ channel assembly. Neuron 11:67–76.
Sheng M, Liao YJ, Jan YN, Jan LY (1993) Presynaptic A-current based on heteromultimeric potassium channels detected *in vivo*. Nature 365:72–75.
Stocker M, Stuhmer W, Wittka R, Wang S, Muller R, Ferrus A, Pongs O (1990) Alternative *shaker* transcripts express either rapidly inactivating or noninactivating K^+ channels. Proc Natl Acad Sci USA 87:8903–8907.
Stuhmer W, Ruppersberg JP, Schroter KH, Sakmann B, Stocker M, Giese KP, Perschke A, Baumann A, Pongs O (1989) Molecular basis of functional diversity of voltage-gated potassium channels in mammalian brain. EMBO J 8:3235–3244.
Stuhmer W, Conti F, Stocker M, Pongs O, Heinemann SH (1991) Gating currents of inactivating and noninactivating potassium channels expressed in *Xenopus* oocytes. Pflügers Arch 418:423–429.
Tejedor FJ, Bokhari A, Rogero O, Gorczyca M, Zhang J, Kim E, Sheng M, Budnik V (1997) Essential role for dlg in synaptic clustering of *shaker* K^+ channels *in vivo*. J Neurosci 17:152–159.
Terlau H, Shon K, Grilley M, Stocker M, Stuhmer W, Olivera B (1996) Strategy for rapid immobilization of prey by a fish-hunting marine snail. Nature 381:148–151.
Tierney AJ, Harris-Warrick RM (1992) Physiological role of the transient potassium current in the pyloric circuit of the lobster stomatogastric ganglion. J Neurophysiol 67:599–609.
Timpe LC, Schwarz TL, Tempel BL, Papazian DM, Jan YN, Jan LY (1988) Expression of functional potassium channels from *Shaker* cDNA in *Xenopus* oocytes. Nature 331:143–145.
Wang H, Kunkel DD, Martin TM, Schwartzkroin PA, Tempel BL (1993) Heteromultimeric potassium channels in the terminal and juxtaparanodal regions of neurons. Nature 365:75–79.
Wei A, Covarrubias M, Butler A, Baker K, Pak M, Salkoff L (1990) K^+ current diversity is produced by an extended gene family conserved in *Drosophila* and mouse. Science 248:599–603.
Woodgett JR, Gould KL, Hunter T (1986) Substrate specificity of protein kinase C: use of synthetic peptides corresponding to physiological sites as probes for substrate recognition requirements. Eur J Biochem 161:177–184.
Wu CF, Haugland FN (1985) Voltage-clamp analysis of membrane currents in larval muscle fibers of *Drosophila*: alteration of potassium currents in *shaker* mutants. J Neurosci 5:2626–2640.
Xu J, Yu W, Jan YN, Jan LY, Li M (1995) Assembly of voltage-gated potassium channels. J Biol Chem 270:24761–24768.
Yellen G, Jurman ME, Abramson T, MacKinnon R (1991) Mutations affecting internal TEA blockade identify the probable pore-forming region of a K^+ channel. Science 251:939–941.
Yool AJ, Schwarz T (1991) Alteration of ionic selectivity of a K^+ channel by mutation of the H5 region. Nature 349:700–704.
Zagotta WN, Aldrich RA (1990) Voltage-dependent gating of *shaker* A-type channels in *Drosophila* muscle. J Gen Physiol 95:29–60.
Zagotta WN, Hoshi T, Aldrich RW (1990) Restoration of inactivation in mutants of *shaker* potassium channels by a peptide derived from *ShB*. Science 250:568–571.